

Optimized FoPID Controller for Doubly-Fed Induction Generator based Wind Turbine using Root Tree Optimization Algorithm

Sumanth Yamparala^{*†} , G.Sambasiva Rao^{**} , N.Dharani Kumar^{***} 

*Department of Electrical and Electronics Engineering, RVR&JC College of Engineering, Guntur, Andhra Pradesh-522019, India.

**Department of Electrical and Electronics Engineering, RVR&JC College of Engineering, Guntur, Andhra Pradesh-522019, India.

***Department of Electrical and Electronics Engineering, RVR&JC College of Engineering, Guntur, Andhra Pradesh-522019, India.

(sumanth46@gmail.com, com, sambasiva.gudapati@gmail.com, dharaninarne@gmail.com)

[†]Corresponding author: Sumanth Yamparala, Department of Electrical and Electronics Engineering, R.V.R. & J.C. College of Engineering, Guntur, Andhra Pradesh-522019, India, Tel:+91 9948198771, sumanth46@gmail.com

Received: 09.10.2023 Accepted:27.11.2023

Abstract- In recent times, there has been a significant increase in wind production, causing extensive research on the regulation of active (P) and reactive power (Q) in wind power systems. Additionally, investigations have been conducted on the quality of power supplied by these systems and their integration with distribution networks. This work presents a novel contribution that employs the Fractional Order Proportional Integral Derivative (FoPID) controller. The primary objective of this study is to develop a field oriented control method for a doubly-fed induction generator (DFIG) based wind system, along with an optimization strategy using the Root Tree Optimization (RTO) algorithm. It is used on both the machine and network sides of the converters. The RTO method is based on analyzing the behavior of trees' underlying foundations as a function of their underground control level in search of subterranean water. The proposed control strategy is evaluated using a MATLAB/Simulink model for shorter settling time, less overshoot in the transient state, as well as a minimal oscillation. The FoPID controller produces better simulation results than the conventional PI regulator. Finally, the superiority of the implemented work is compared and proved over the conventional model.

Keywords DFIG, FoPID controller, Rotor Side Converter, RTO algorithm.

Nomenclature

AI	Artificial Intelligence	PI	Proportional–Integral
ACO	Ant colony optimization	PID	Proportional–Integral–Derivative
BSC	Backstepping Control	PSO	Particle Swarm Optimization
DFIG	Doubly Fed Induction Generator	RTO	Root Tree Optimization
FOCs	Fractional order Controllers	RSC	Rotor Side Converter
FoPID	Fractional Order Proportional Integral Derivative	SA	Simulated annealing
GA	Genetic algorithm	SM	Sliding Mode
GSC	Grid Side Converter	THD	Total Harmonic Distortion
GSO	Gravitational swarm optimizer	VSWT	Variable Speed Wind Turbine
NN	Neural Network	WECS	Wind Energy Conversion System
VC	Vector Control	WT	Wind Turbine

1. Introduction

Nowadays, environmental pollution concerns cannot be overlooked, especially in light of climate change, which is affecting a large number of people all over the world. Several researchers suggest these changes in the environment are mostly the result of releases of greenhouse gases, especially CO₂, which are also responsible for warming the planet and raising temperatures globally. Natural catastrophes, according to experts, pose an unparalleled ecological danger to ecosystem stability, and a rapid transition to renewable energy supplies is strongly recommended [1]. Wind energy is a clean, cost-effective, renewable, and environmentally friendly source of energy, making it one of the most promising and vital types of renewable energy in the world [2]. In small-scale residential applications of wind turbines (WT), the most common types of generators employed are synchronous generators (SG) and squirrel cage induction generators (SCIG). However, Doubly Fed Induction Generators (DFIG) are commonly utilized in wind turbines with megawatt-level capacity [3]. In the DFIG configuration, the rotor winding is electrically coupled to the rotor-side converter (RSC), whereas the stator is directly interconnected to the power grid [4]. Over the past few decades, a substantial amount of research has been devoted to examining the fault-tolerance capability, control methods, and optimal operation of doubly-fed induction generator-based wind turbines (DFIG-WTs) connected to the AC grid [5-6]. Induction generators may be effectively regulated by many methods, including field-oriented control and indirect torque control. These approaches primarily aim to efficiently control the DFIG's P and Q [7]. The conventional vector control approach is commonly employed in many practical applications for operating induction machines, because to its basic design and simplicity of implementation [8-9]. Nevertheless, it possesses significant drawbacks. A primary constraint of this control methodology is its dependence on the parameters of conventional PI/PID controllers, which significantly impacts the efficacy of the vector control technique. However, in a complex system with variable unpredictability, the gains of the PI/PID controllers are generally modified arbitrarily and manually utilizing very complicated, tedious, and time-consuming procedures [10-11]. Sliding mode control (SMC) and backstepping (BSC) are contemporary control strategies that can be utilized in instead of field oriented control to improve the robustness of the WECS. These sophisticated control techniques have the potential to enhance the overall efficacy of DFIG-based wind turbine systems [12-15]. Due to its potential to provide better control performance than integer order controllers in many real-world scenarios, fractional-order controllers, or FOCs, have gained popularity in recent times [16]. FOCs have drawn a lot of interest due to their ability to depict the non-linear dynamics of complex systems [17]. Complex systems that cannot be described by integer order systems may also be simulated using them [18]. Because of this, FOCs may be used to improve response time and stability in existing control systems. Due to the difficulty of tuning FOCs using traditional approaches, contemporary techniques have been used to optimize FOC parameters depending on multiple factors such

as stability, robustness, and performance. In recent years, some research studies have employed novel methodology such as artificial intelligence (AI) techniques [19-20]. Numerous studies and investigations were conducted to reduce the harmonics in rotor current and address the issue of chattering in both the P and Q of the DFIG. To regulate the converter, sliding mode regulators were used in different control systems [21-22]. Further studies have improved control performance using a range of AI methodologies and random search methods. PID controllers have been efficiently optimized using fuzzy systems, PSO, and NNs. [23-24]. Modern optimization techniques that have shown their effectiveness in FOCs optimization include metaheuristic approaches. These approaches make use of sophisticated optimization algorithms that conduct their searches using a random-search methodology. The algorithms include Genetic algorithms (GA) [25], Simulated annealing (SA) [26], Ant colony optimization (ACO) [27], Particle swarm optimization (PSO) [28], Gravitational swarm optimizer (GSO) [29]. Recent studies [30-31] have investigated the application of nature-inspired and bio-inspired optimization approaches to enhance the control behavior of power systems. Metaheuristic algorithms draw inspiration from several natural events, including animal behavior that have been proposed and discussed in recent literature [32-35].

The contribution of proposed method is given below:

1. An effective FoPID controller decreases settling time, has less overshoot in the transient state, and has a low steady-state oscillation in DFIG (less overshoot, faster reaction time, less power ripples, and lower THD).
2. Presents a Root Tree Optimization approach for optimizing the gain parameters of the FoPID controller.

The paper is organized as follows: Section II covers the proposed DFIG-based WT modeling, Section III demonstrates an improved FoPID controller utilizing the root tree optimization technique, Section IV examines the findings, and Section V concludes the work.

2. Proposed DFIG Based Wind Turbine Modelling

The grid connected DFIG based WT is shown in Fig.1. The stator is required to be connected to the network directly in DFIG, whereas the rotor should be connected to the RSC [36-37].

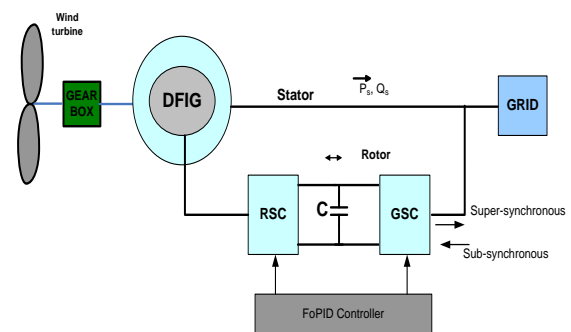


Fig. 1. DFIG based WECS.

Voltage Equations:

$$V_{ds} = R_s I_{ds} + \omega_s \psi_{qs} \quad (1)$$

$$V_{qs} = R_s I_{qs} - \omega_s \psi_{ds} \quad (2)$$

$$V_{dr} = R_r I_{dr} + \frac{d\psi_{dr}}{dt} - s\omega_s \psi_{qr} \quad (3)$$

$$V_{qr} = R_r I_{qr} + \frac{d\psi_{qr}}{dt} + s\omega_s \psi_{dr} \quad (4)$$

Flux Equations:

$$\psi_{ds} = L_s I_{ds} + M I_{dr} \quad (5)$$

$$\psi_{qs} = L_s I_{qs} + M I_{qr} \quad (6)$$

$$\psi_{dr} = L_r I_{dr} + M I_{ds} \quad (7)$$

$$\psi_{qr} = L_r I_{qr} + M I_{qs} \quad (8)$$

POWER EQUATIONS:

$$P_s = V_{ds} I_{ds} + V_{qs} I_{qs} \quad (9)$$

$$Q_s = V_{qs} I_{ds} - V_{ds} I_{qs} \quad (10)$$

$$P_r = V_{dr} I_{dr} + V_{qr} I_{qr} \quad (11)$$

$$Q_r = V_{qr} I_{dr} - V_{dr} I_{qr} \quad (12)$$

TORQUE EQUATIONS:

$$T_e = -\frac{3P}{2} \frac{(\psi_{ds} I_{qs} - \psi_{qs} I_{ds})}{2} \quad (13)$$

Where R_s, R_r, R_r, L_s and L_r denotes resistance, inductance of stator and rotor windings respectively. Direct and quadrature components of stator and rotor voltage are represented with $V_{ds}, V_{qs}, V_{dr}, V_{qr}$. $I_{ds}, I_{qs}, I_{dr}, I_{qr}$ denotes direct and quadrature components of stator and rotor currents. $\psi_{ds}, \psi_{qs}, \psi_{dr}, \psi_{qr}$ represents direct and quadrature components of stator and rotor flux. P is the number of poles.

2.1. Rotor Side Converter Control Strategy

This section addresses the idea behind the VC method for controlling the power of DFIG-based WTs. As shown in Fig.2, the d and q axes are used to change the P and Q dealt between the DFIG generator and grid [38–39].

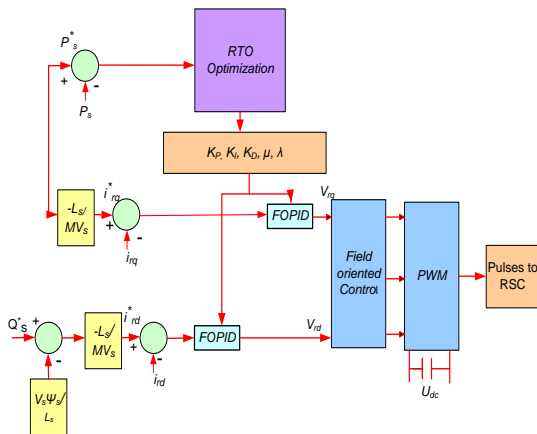


Fig. 2. RSC control structure.

$$\psi_{ds} = \psi_s \quad (14)$$

$$\psi_{qs} = 0$$

$$V_{ds} = 0 \quad (15)$$

$$V_{qs} = \omega_s \psi_{ds}$$

$$T_e = P \frac{L_m}{L_s} (I_{rq} \psi_{sd}) \quad (16)$$

$$V_{dr} = R_s I_{dr} + \sigma L_r \frac{dI_{dr}}{dt} - g \sigma \omega_s L_r I_{qr} \quad (17)$$

$$V_{qr} = R_s I_{qr} + \sigma L_r \frac{dI_{qr}}{dt} + g \sigma \omega_s L_r I_{dr} + g \frac{L_m V_s}{L_s}$$

$$P_s = -V_s \frac{L_m}{L_s} I_{qr} \quad (18)$$

$$Q_s = -\frac{V_s L_m}{L_s} I_{dr} + \frac{V_s \psi_s}{L_s}$$

$$\sigma = 1 - \frac{L_m^2}{L_s L_r} \quad (19)$$

$$g = \frac{(\omega_s - \omega_r)}{\omega_s} \quad (20)$$

The rotor reference currents are

$$I_{dr}^* = \frac{V_s}{L_m \omega_s} - \frac{L_s}{L_m V_s} Q_s^* \quad (21)$$

$$I_{qr}^* = -\frac{L_s}{L_m V_s} P_s^* \quad (22)$$

The P and Q generated are regulated in the d and q axes via two independent loops [40].

2.2. Grid Side Converter Control Strategy

Figure 3 depicts the GSC control structure. A VC approach is often used to regulate the GSC in combination with the grid voltage orientation [41].

The voltage across the DC capacitor is written as:

$$V_{dc}^* = V_{dc-meas} + \frac{1}{C_{dc}} \int_0^t i_{dc} dt \quad (23)$$

$$= V_{dc-meas} + C^* \frac{1}{C_{dc}} \int_0^t (i_{dc_GSC} - i_{dc_RSC}) dt \quad (24)$$

The DC current flowing into or out of the GSC and RSC is represented by i_{dc_GSC} and i_{dc_RSC} , respectively. In this part, switching signals are created by comparing measured network currents to reference network currents using a hysteresis controller [42].

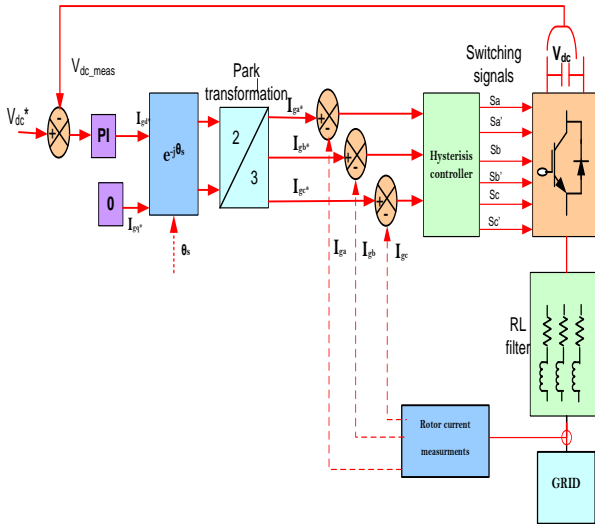


Fig.3. GSC Control structure.

3. Optimized FoPID Controller via Root Tree Optimization Algorithm

3.1. Optimized FoPID Control

Proposed RTO optimization technique optimizes the gain parameters of the FoPID controller, which determines the controller parameters of the DFIG based on quadrature rotor current error linked to P and direct rotor current error linked to Q [43]. An overview of differentiation and integration is provided by fractional-order calculus and Eq. (25)

demonstrates the formulation of the basic operator ${}_a W_t^\alpha$, here $\alpha \in \mathfrak{R}$ point out the order of operation while t and a point out upper and lower limits [44].

$${}_a W_t^\alpha = \begin{cases} \frac{d^\alpha}{dt^\alpha}, & \alpha > 0 \\ 1, & \alpha = 0 \\ \int_a^t (d\tau)^{-\alpha} & \alpha < 0 \end{cases} \quad (25)$$

Eq. (26) depicts the RL description [45] that employs the Gamma function $\Gamma(\cdot)$, in which n refer to 1st integer that was larger than operation order α . In addition, Eq. (27) specifies the RL description for FoPID.

$${}_a W_t^\alpha f(t) = \frac{1}{\Gamma(n-\alpha)} \frac{d^n}{dt^n} \int_a^t \frac{f(\tau)}{(t-\tau)^{\alpha-n+1}} d\tau \quad (26)$$

$${}_a W_t^\alpha f(t) = \frac{1}{\Gamma(\alpha)} \int_a^t (t-\tau)^{\alpha-1} f(\tau) d\tau \quad (27)$$

The Laplace transformation of Eq. (26) is specified in Eq. (28), here $\ell\{\cdot\}$ stand for the Laplace operator.

$$\int_0^\infty {}_a W_t^\alpha f(t) e^{-st} dt = s^\alpha \ell\{f(t)\} - \sum_{K=0}^{n-1} s^K {}_a W_t^{\alpha-K-1} f(t) \Big|_{t=0} \quad (28)$$

The transfer function of FoPID controller is indicated in Eq. (29), here k_p , k_i as well as k_d denotes proportional, integral and derivative gain correspondingly. In addition, λ and μ point out the fractional integrator and differentiator orders correspondingly.

$$Y(s) = k_d + \frac{k_i}{s^\lambda} + k_p s^\mu \quad (29)$$

3.2. Objective Function and Solution Encoding

The goal of the paper is to model a FoPID controller for a low damping plant as shown in fig.4. The DFIG plant's 6th order transfer function model is shown in Eq. (30).

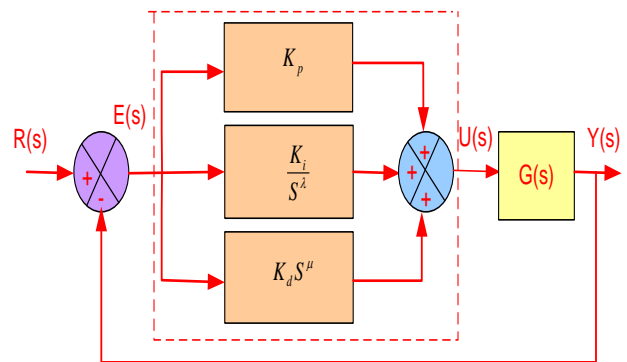


Fig.4. FoPID controller structure

$$G(s) = \frac{0.000324s^6 - 1.75s^5 - 2366s^4 + 7.9e^6 s^3 + 7.5e^9 s^2 + 5e^{12} s + 2.18e^{14}}{s^6 + 2340s^5 + 8.67e^6 s^4 + 4.79e^9 s^3 + 2.7e^{12} s^2 + 1.27e^{14} s + 9.6e^{14}} \quad (30)$$

The CLTF for the current loop is

$$\frac{I_{rd(rq)}}{I_{rd(rq)}^*} = \frac{G(s)}{1 + G(s)} \quad (31)$$

The fitness function is:-

$$F = (1 - e^{-\beta})(M_p + e_{ss}) + (e^{-\beta})(T_s - T_r) \quad (32)$$

$$Ob = \text{Min}(F) \quad (33)$$

In order to achieve optimum control, the FoPID parameters are optimally set using a novel RTO model. Figure 4 depicts the solution provided by the implemented technique

in which k_d , k_i and k_p , λ , μ are the gain parameters FoPID controller.

3.3. Proposed RTO Algorithm

Building the bases and facilities for trees' underground root systems-connected roots has transformed into a modern technology due to the social behavior of the roots. [46]. After discovery of this approach, trees are no longer merely a way of beautifying the surroundings; they now play a vital function thanks to their root behavior, which has been turned into an AI technique [47]. This demonstrates how plants have altered tree roots' algorithm in their hunt for subsurface water. The first knot in the tree gives a path for searching for other roots. It is the first collection of random solutions [48]. The roots in the first collection that are the most fit and closest to the goal are evaluated, and the roots that are the most distant from the goal are discarded. Before continuing the search, the stop condition (number of iterations) is confirmed. If the maximum number of duplicates is not attained, the answer is to obtain the ideal fitness level. [49].

Water Detector (roots):

As tree roots rely on their behavior to decide the best or nearest location to convey water, they might be regarded of as subterranean water detectors. The hunt for water starts at the top knot of the tree stem, which provides us roots in the top layer of the ground (first generation). The root closest to the wetness degree generates the knot from which the generation forks and seeks the ideal area to offer water once more. The latter then go out on a haphazard search for water [50]. Fig. 5 depicts the Water searching pattern of Roots.

This technique was developed using the idea of how tree roots search for subterranean water in relation to the thickness of the earth's crust. This characteristic allows us to develop a novel algorithm. Variables must be explained before this algorithm can be used.

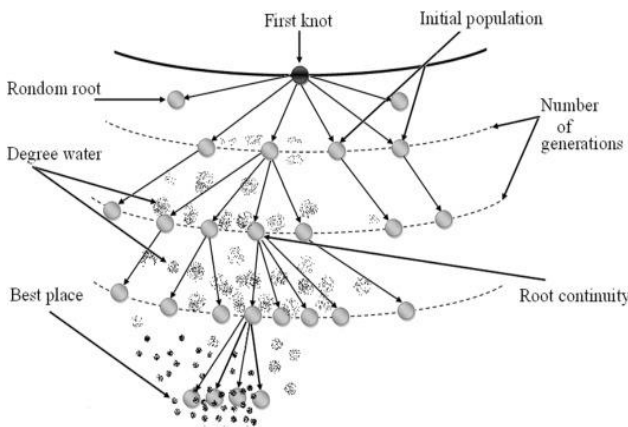


Fig.5. Water searching pattern of Roots.

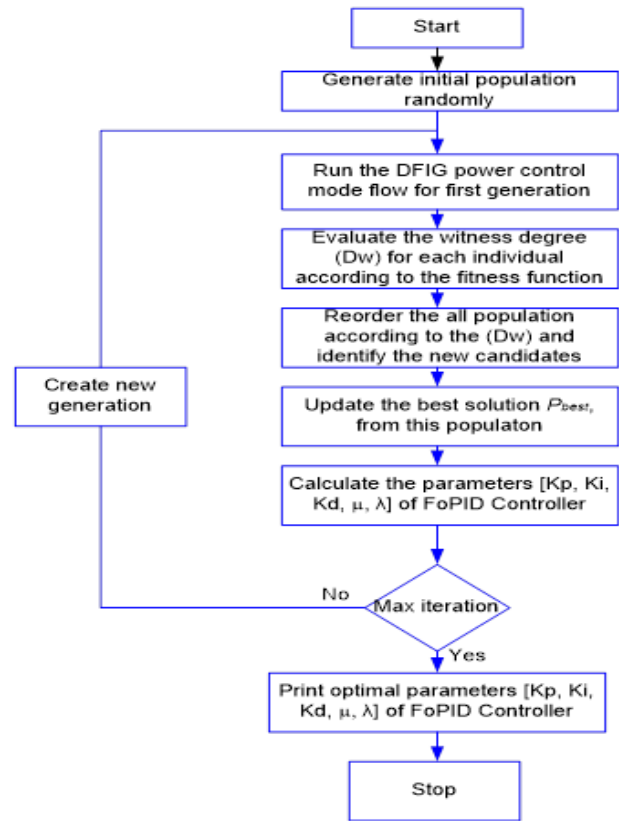


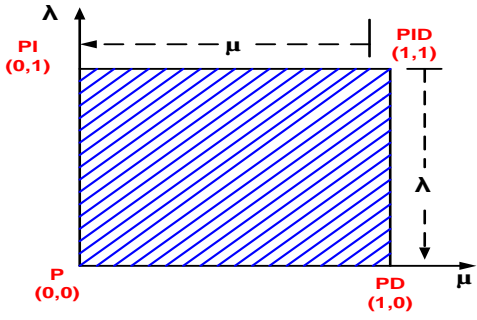
Fig. 6. Flowchart of RTO FoPID controller.

RTO Parameters.

Parameters	Value
Size	20
Number of iterations	20
b1=b2=b3	2
Rr=Rn	0.3
Rc	0.4
dim	2

4. Results and Discussion

In order to evaluate the efficacy of the proposed method, a wind farm with a capacity of 9 MW and a DFIG driven by a wind turbine is taken into consideration. The system consists of six 1.5 MW wind turbines that are interconnected with a grid through a feeder. The performance of the proposed method employing RTO + FoPID controller was evaluated using the MATLAB/SIMULINK environment. This section presents an analysis of the results obtained from the simulation performed for the proposed method. The strategy that was proposed was thoroughly evaluated, and its superiority over the traditional method was demonstrated.



The analysis on gain parameters (k_d, k_i and k_p, λ, μ) of the FoPID controller is demonstrated in this section. Fig. 8 shows the gain values attained by the presented work with respect to iterations.

Fig. 7. Operating range of FoPID controller

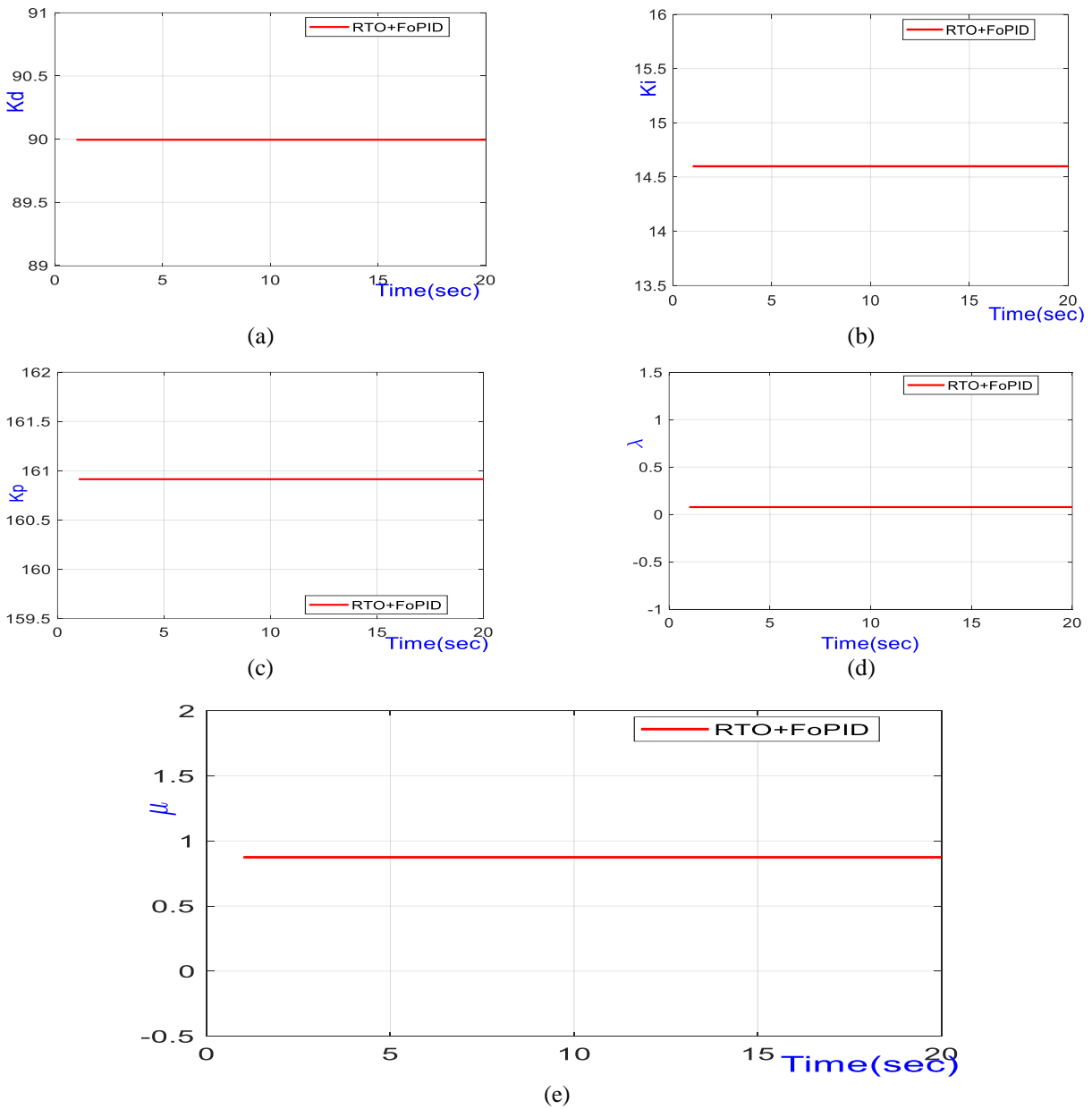


Fig. 8. Gain analysis of implemented approach (a) k_d (b) k_i (c) k_p (d) λ and (e) μ

Analysis on Rotor Current

Fig. 9 illustrates the study of the rotor current for the proposed RTO + FoPID model over PI controller with respect to time. Upon analysis of the graph, it can be shown that the rotor current obtained by the proposed model exhibits minimal fluctuations in comparison to previous approaches.

Furthermore, the developed RTO model efficiently regulates the maximum permissible rotor current within a range of ± 1.5 per unit. Consequently, the occurrence of over currents in the RSC is eliminated in the event of symmetric grid failures. When examining the traditional approaches, it is evident that the current of the rotor exceeds ± 1.5 per unit (pu) and so violates the criterion for low voltage ride-through (LVRT).

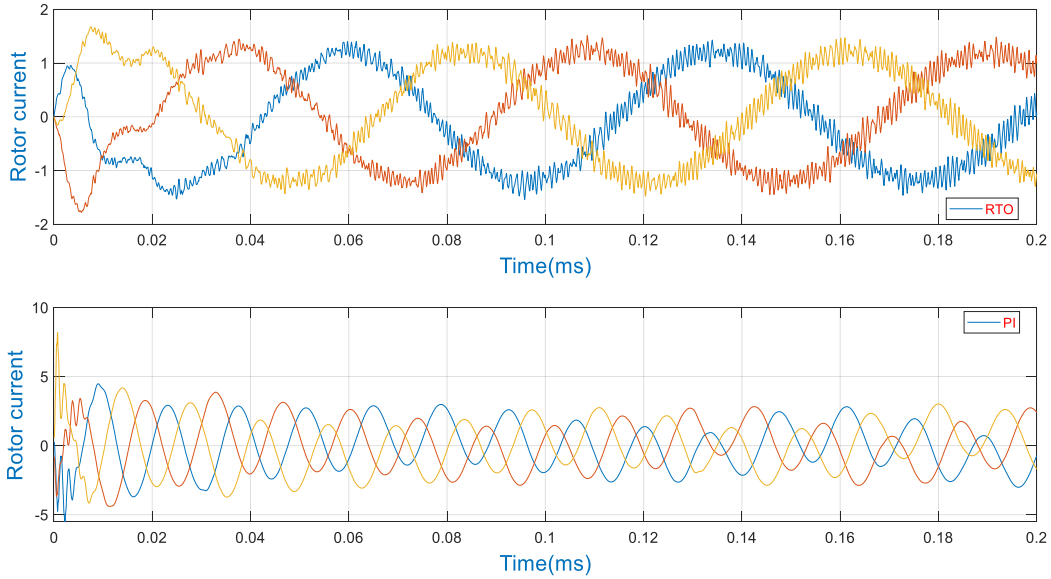


Fig. 9. Rotor Current Analysis of adopted and existing model (a) RTO+ FoPID (b) PI

Stator Power Analysis

Figure 10 presents the comparison between the stator P and Q achieved by the RTO + FoPID model and the conventional model over a period of time. On observing Fig. 10(a), the stator active power attained by the proposed model as well as compared models is found to be increasing with increase in time. However, the RTO model has accomplished higher stator active power value than the proposed model, but,

this variation can be considered negligible as the proposed model satisfies LVRT condition in a better way. In Fig. 10(b), the stator Q is minimized with increase in time; however, the proposed model has attained a higher value than the compared models. Thus, the enhancement of the adopted model in attaining better LVRT capability is proved.

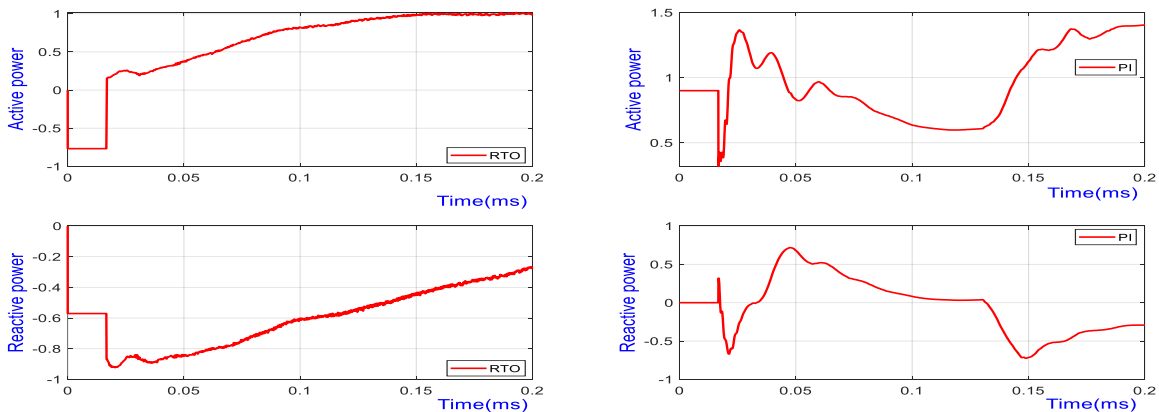


Fig. 10. Analysis on (a) stator P and (b) stator Q attained by proposed and existing model.

Analysis on Stator Current

The stator current analysis for the proposed RTO + FoPID model compared to conventional method is shown in Fig. 11. Based on the results obtained, it can be concluded that the proposed method successfully meets the Low Voltage Ride Through (LVRT) requirements, as shown by the stator current

remaining within the range of ± 1.5 per unit (pu). In contrast, conventional method surpass this limit and fail to comply with the necessary LVRT criteria. Furthermore, the stator current oscillations achieved using the model described in this study exhibit low amplitude.

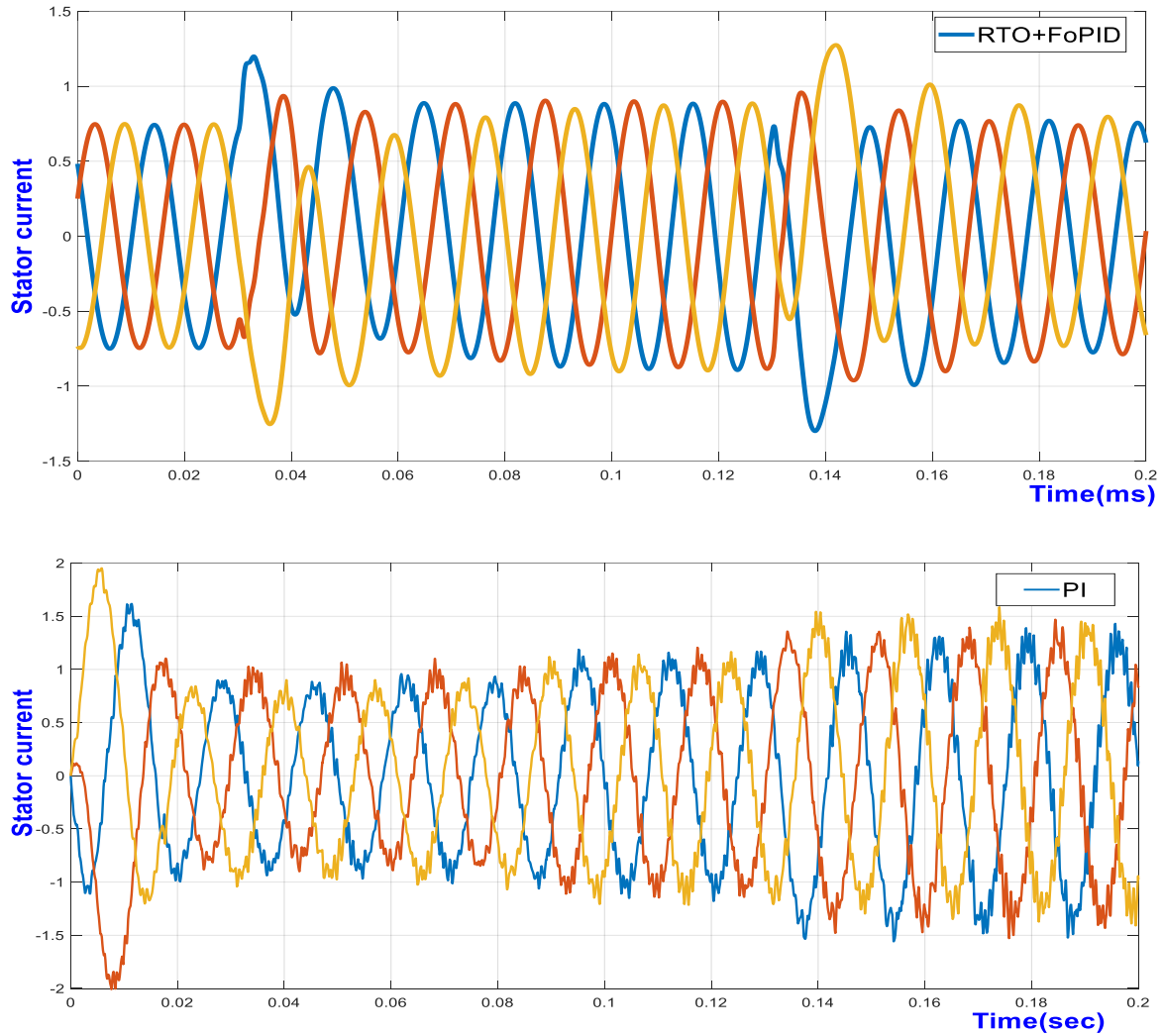


Fig. 11. Stator Current Analysis for proposed model and PI controller.

Steady State Response

Table 1 presents the steady state response of the proposed controller and conventional controller. Upon observation of

the results, it can be seen that the RTO + FoPID model has achieved a shorter rising time and settling time compared to the PI controller.

Table 1. Steady state analysis

Methods	Rise Time (sec)	Settling Min (sec)	Settling Max (sec)	Overshoot (sec)	Undershoot (sec)	Peak (sec)	Peak Time (sec)
RTO + FoPID	0.01129	0.8027	0.8694	0	0	0.8694	1.3136
PI	0.1313	0.9023	0.9575	0	0	0.9575	1.4498

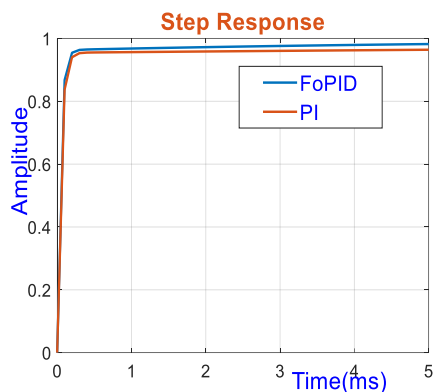


Fig. 12. Step response of DFIG for RTO + FoPID controller, PI controller.

THD Analysis

The THD analysis for the proposed RTO + FoPID scheme and existing model is summarized in Table 2. The THD of the proposed scheme should be minimal for the better controller performance. While analysing the outcomes the adopted scheme has accomplished a least THD value of 3.94%. THD of rotor current using RTO + FoPID controller is shown in Fig. 13. In addition, the optimally attained gain parameters for the implemented model and existing models are revealed in Table 3.

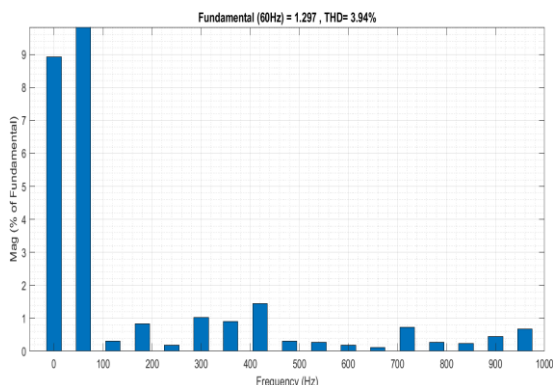


Fig. 13. THD of the rotor current using RTO + FoPID controller.

Table 2. THD analysis of proposed model and existing model

Method adopted	% THD
PI controller	8.67
RTO + FoPID	3.94

Table 3. Analysis on optimal gain parameters attained by implemented model and existing models

Gain parameters	RTO + FoPID
k_p	160.91
k_i	14.6
k_d	89.995
μ	0.87516
λ	0.077516

5. Conclusion

This study investigates the efficacy of a new control approach, the Root Tree optimization (RTO) combined with the FoPID controller, for DFIG connected WECS. The study considers the inclusion of conventional PI and RTO + FoPID controller. The findings indicate that the RTO + FoPID controller exhibits superior performance compared to the conventional PI controller. This is achieved through the optimization of various controller gain parameters. The RTO + FoPID controller successfully reduces the harmonics in the rotor current of the DFIG to a level of 3.94%. Specifically, the RTO + FoPID controller that has been suggested demonstrates a decrease in rising time to 1.129 μ s and settling time to 9.027 μ s. In contrast, the standard PI controller exhibit higher specifications. The integration of the RTO combined with the FoPID controller ensured increased performance of the DFIG based WECS as seen by the enhanced steady state responsiveness. Thus, the enhancement of the presented RTO + FoPID scheme has been validated effectively.

References

- [1] F. Abdoune, D. Aouzellag and K. Ghedamsi, “Terminal voltage build-up and control of a DFIG based stand-alone wind energy conversion system”, *Renewable Energy*, Vol. 97, pp.468–480, 2016, 10.1016/j.renene.2016.06.005.
- [2] N.Dharani Kumar, T.A. Ramesh Kumar, A. Rama KoteswaraRao, “Effect of Partial Shading on the Performance of Various 4x4 PV Array Configurations” *ECTI Transactions on Electrical Engineering, Electronics and Communications*, vol. 20, no. 3, pp. 427–437, 2022.
- [3] R. Aubree, A. François, M. Michel and L. Loron, “Design of an efficient small wind-energy conversion system with an adaptive sensorless MPPT strategy”, *Renewable Energy*, 86, 280-291, 2016. DOI:10.1016/j.renene.2015.07.091, 86, 2016, 280-291.
- [4] A. Azzouz, B. Abdelhamid, “Performance of PI controller for control of active and reactive power in DFIG operating in a grid-connected variable speed wind energy conversion system”, *Front Energy*, 8(3):371– 8, 2014, DOI: 10.1007/s11708-014-0318-6.
- [5] A. Akhbari, M. Rahimi, M.H. Khooban, “Various control strategies performance assessment of DFIG wind turbine connected to a DC grid”. *IET Electr. Power Appl.* 17(5), 687–708, 2023.
- [6] J. Nikolaos, E. Tsioumas, C. Mademlis, and A. Evgeny Solomin, “Highly effective fault-ride-through strategy for a wind energy conversion system with a doubly fed induction generator” *IEEE Transactions on Power Electronics* 35, no. 8, 8154-8164, 2020.
- [7] A. Chebel, A. Benretem, I. Dobrev, and B. Barkati, “Comparative study of two control strategies proportional integral and fuzzy logic for the control of a doubly fed induction generator dedicated to a wind application”

- International Journal of Power Electronics and Drive Systems 11, no. 1, 263, 2020.
- [8] S. Ghodelbourk, D. Dib, A. Omeiri and A.T. Azar, "A MPPT control in wind energy conversion systems and the application of fractional control ($PI\alpha$) in pitch wind turbine", *International Journal of Modelling, Identification and Control*, Vol. 26, No. 2, pp.140–151, 2016.
- [9] A. M. Kassem, K. M. Hasaneen, A. M. Yousef, "Dynamic modelling and robust power control of DFIG driven by wind turbines at infinite grid", *International Journal of Electrical Power & Energy Systems*, 44(1), pp. 375–382, 2013, <https://doi.org/10.1016/j.ijepes.2011.06.038>
- [10] Z. Zeghdi, L. Barazane, A. Larabi, "Field Oriented Control of Doubly Fed Induction Generator Integrated in Wind Energy Conversion System Using Artificial Neural Networks", In: 2018 International Conference on Electrical Sciences and Technologies in Maghreb (CISTEM), Algiers, Algeria, pp. 1–7, 2018. <https://doi.org/10.1109/CISTEM.2018.8613558>
- [11] Y. Bekakra, D. B. Attous, "Optimal tuning of PI controller using PSO optimization for indirect power control for DFIG based wind turbine with MPPT", *International Journal of System Assurance Engineering and Management*, 5(3), pp. 219–229, 2014. <https://doi.org/10.1007/s13198-013-0150-0>.
- [12] M. Ali, S. M. Amr and M. Khalid, "Speed control of a wind turbine–driven doubly fed induction generator using sliding mode technique with practical finite-time stability". *Front. Energy Res.* 10, 970755, 2022. DOI:10.3389/fenrg.2022.970755.
- [13] Y. Mousavi, G. Bevan, I. B. Kucukdemiral and A. Fekih, "Sliding mode control of wind energy conversion systems: trends and applications". *Renew. Sustain. Energy Rev.* 167, 112734, 2022. doi:10.1016/j.rser.2022.112734.
- [14] D. Ismail, A. El Fadili, C. Berrahal, R. Lajouad, A. El Magri, F. Giri, A. Taher Azar, and S. Vaidyanathan, "Adaptive backstepping controller for DFIG-based wind energy conversion system", In *Backstepping control of nonlinear dynamical systems*, pp. 235-260, Academic Press, 2021.
- [15] H. Choja, A. Derouich, T. Hallabi, O. Zamzoum, M. Taoussi, S. Rhaili, and O. Boukhrachef, "Performance improvement of the variable speed wind turbine driving a DFIG using nonlinear control strategies" *International Journal of Power Electronics and Drive Systems (IJPEDS)* 12, no. 4, 2470-2482, 2021, DOI:10.11591/ijpeds.v12.i4.pp2470-2482.
- [16] R.A.Z. Daou, X. Moreau, "Comparison between integer order and fractional order controllers", In *Proceedings of the MELECON 2014-2014 17th IEEE Mediterranean Electrotechnical Conference*, Beirut, Lebanon, 13–16 April 2014; pp. 292–297.
- [17] R. Caponetto, J.T. Machado, E. Murgano, M.G. Xibilia, "Model Order Reduction: A Comparison between Integer and Non-Integer Order Systems Approaches", *Entropy*, 21, no.9, 876, 2019.
- [18] M. Al-Dhaifallah, A.M. Nassef, H. Rezk, K.S. Nisar, "Optimal parameter design of fractional order control based INC-MPPT for PV system", *Solar Energy*, 159, 650–664, 2018.
- [19] R. Marouane, Z. Malika, "Particle swarm optimization for tuning PI controller in FOC chain of induction motors", In: 2018 4th International Conference on Optimization and Applications (ICOA), Mohammedia, Morocco, pp.1–5, 2018, <https://doi.org/10.1109/ICOA.2018.8370512>.
- [20] N. K. Bahgaat, M. M. Hassan, "Swarm Intelligence PID Controller Tuning for AVR System", In: Azar, A. T., Vaidyanathan, S. (eds.) *Advances in Chaos Theory and Intelligent Control*, Springer, Cham, Switzerland, 2016, pp. 791–804. https://doi.org/10.1007/978-3-319-30340-6_33.
- [21] Z. Zeghdi, L. Barazane, A. Larabi, A. Samir, K. Khechiba, "Artificial Neural Networks (ANNs)-Based Robust Tracking Control for DFIG integrated in WECS", In: 2018 International Conference on Applied Smart Systems (ICASS), Medea, Algeria, 2018, pp. 1–6. <https://doi.org/10.1109/ICASS.2018.8652023>.
- [22] Y. Sumanth, L. Lakshminarasimman, and G. Sambasiva Rao, "Improvement of LVRT Capability for DFIG based WECS by Optimal Design of FoPID Controller using SLnO+ GWO Algorithm", *International Journal of Intelligent Engineering & Systems*, 16.1 (2023).
- [23] N.Dharani Kumar, T.A. Ramesh Kumar, A. Rama KoteswaraRao "Evaluation of SP-CT PV Array Configuration Performance with Maximum Power Point Tracking Techniques under Partial Shading Conditions", *Clean Energy*, vol. 7, no. 3, pp. 620–634, 2023.
- [24] N.Dharani Kumar, T.A. Ramesh Kumar, A. Rama KoteswaraRao "Traditional and hybrid solar photovoltaic array configurations for partial shading conditions: perspectives and challenges", *Bulletin of Electrical Engineering and Informatics*, vol. 12, no. 2, pp. 642-649, 2023.
- [25] J.H. Holland, "Genetic Algorithms", *Scientific american*, 1992, 267, 66–73.
- [26] P.M. Pardalos, T.D Mavridou, Floudas, C.A. Pardalos, P.M. Eds, "Simulated Annealing. In *Encyclopedia of Optimization*" Springer: Boston, MA, USA, 2009; pp. 3591–3593.
- [27] M. Dorigo, M. Birattari, T. Stutzle, "Ant colony optimization" *IEEE Comput. Intell. Mag.* 2006, 1, 28–39.
- [28] J. Kennedy, R. Eberhart, "Particle swarm optimization" In *Proceedings of the ICNN'95-International Conference on Neural Networks*, Perth, Australia, 27 November–1 December 1995; pp. 1942–1948.

- [29] A. Yadav, K. Deep, J.H. Kim, A.K. Nagar, "Gravitational swarm optimizer for global optimization", *Swarm Evol. Comput.* 2016, 31, 64–89.
- [30] A. Lakhdara, B. Tahar and M. Abdelkrim, "Sliding mode control of doubly-fed induction generator in wind energy conversion system", 2020 8th International Conference on Smart Grid (icSmartGrid). IEEE, 2020 DOI: 10.1109/icSmartGrid49881.2020.9144778.
- [31] P. Indranil, S. Das, and A. Gupta, "Tuning of an optimal fuzzy PID controller with stochastic algorithms for networked control systems with random time delay", *ISA transactions* 50.1 (2011): 28-36 DOI: 10.1016/j.isatra.2010.10.005
- [32] V. Matin, A. Mohammadi, D. Lewis, J. F. Eastham and D. M. Ionel, "Coreless axial flux halbach array permanent magnet generator concept for direct-drive wind turbine", In 2023 12th International Conference on Renewable Energy Research and Applications (ICRERA), pp. 612-617. IEEE, 2023.
- [33] X-S. Yang, "Firefly algorithm, stochastic test functions and design optimisation", *International Journal of Bio-Inspired Computation*, 2(2), pp. 78–84, 2010. <https://doi.org/10.1504/IJBIC.2010.032124>
- [34] Y. Sumanth, L. Lakshminarasimman, and G. Sambasiva Rao. "Optimal design of FoPID controller for DFIG based wind energy conversion system using Grey-Wolf optimization algorithm" *International Journal of Renewable Energy Research (IJRER)* 12.4 (2022): 2111-2120.
- [35] N.Dharani Kumar, T.A. Ramesh Kumar, A. Rama KoteswaraRao, "A Novel PV Array Configuration for Enhancing the Maximum Power from PV Array" *Clean Energy*, vol. 6, Issue 6, pp. 817–826, 2022.
- [36] M. Tazil, V. Kumar, R. C. Bansal, S. Kong, Z. Y. Dong, W. Freitas, and H. D. Mathur. "Three-phase doubly fed induction generators: an overview" *IET Electric Power Applications* 4, no. 2 (2010): 75-89.
- [37] J. Bhola, K. Ram Mohan Rao and Y. Sumanth. "Detailed Dynamic Modeling and Vector Control of Doubly Fed Induction Generator." *International Journal of Applied Engineering Research* 5.10 (2010): 1765-1778.
- [38] K. Kerrouche, A. Mezouar and K. Belgacem, "Decoupled Control of Doubly Fed Induction Generator by Vector Control for Wind Energy Conversion System," in *Overview of renewable energies exploitation in Algeria*, *Energy Procedia*, 2013, vol. 42, pp. 239-248.
- [39] E. J. Kretschmann, J. Fortmann, S. Mueller-Engelhardt, H. Wrede, "Modeling of wind turbines based on doubly-fed induction generators for power system stability studies", *IEEE Trans Energy Convers.* 22, 909–919 (2007).
- [40] E. Aydin, A. Polat and L. T. Ergene, "Vector Control of DFIG in Wind Power Applications," in *IEEE (ICRERA)*, Birmingham, Nov. 2016, pp. 478-483.
- [41] K. Sarah, R. Uhumwangho and K. Okedu. *Harnessing Solar and Wind Power for Hybrid Stand-alone Energy System: The Case of Coastline Communities in Delta State of "Southern Nigeria"*, *International Journal of Smart Grid*, 7, no. 1, pp : 25-37, 2023.
- [42] W. Yuan-Kang and Wu-Han. Yang, "Different control strategies on the rotor side converter in DFIG-based wind turbines" *Energy Procedia* 100 (2016): 551-555 DOI:10.1016/j.egypro.2016.10.217.
- [43] A. Benamor, M. T. Benchouia, K. Srairi, and M. E. H. Benbouzid. "A new rooted tree optimization algorithm for indirect power control of wind turbine based on a doubly-fed induction generator" *ISA transactions* 88 (2019): 296-306.
- [44] B. Amlan, S. Mohanty and R. Sharma, "Ameliorating the FOPID (PI λ D μ) controller parameters for heating furnace using optimization techniques" *Indian journal of science and technology* 9.39 (2016).
- [45] B. Fatiha, I. Colak, A. Bekraoui, K. Roummani and A. Harrouz, "Comparative study between the sliding mode and backstepping current control of a grid-connected direct drive Wind-PMSG system" In 2023 11th International Conference on Smart Grid (icSmartGrid), pp. 1-10. IEEE, 2023.
- [46] L. Fern Ow, E. Koon Sim, "Detection of urban tree roots with the ground penetrating radar Plant", *Biosystems - An International Journal Dealing with all Aspects of Plant Biology: Official Journal of the Societa Botanica Italiana*, vol. 146, pp. 288–297, 2012.
- [47] S. Zhang, J. Yang, "Analysis of User Critical Interests Based on an Improved Shortest Root Tree Algorithms", *IEEE* , 978-1-4244-6789-1/10, 2010.
- [48] Y. Labbi, D. Ben Attous, Hossam, A. Gabbar, B. Mahdad, A. Zidan, "A new rooted tree optimization algorithm for economic dispatch with valve-point effect", *Electrical Power and Energy Systems*, vol. 79, pp. 298–311, 2016.
- [49] D. Lei, Z. Pan, Y. Su and W. Cong, "Splitting and islanding of networked dispersed generators", *Electr Power Autom Equip* 27, no. 7, 2007, 25-29.
- [50] Y. Vishkin, U. Shiloachand and Y. Shiloach, "An O (log n) parallel connectivity algorithm", *J. algorithms*, 3, 1982, 57-67.